Vol. 528: 87–99, 2015
doi: 10.3354/meps11253

MARINE ECOLOGY PROGRESS SERIES
Mar Ecol Prog Ser

Published May 28

Modeling krill aggregations in the central-northern California Current

Jeffrey G. Dorman[1,2,*], William J. Sydeman[1], Marisol García-Reyes[1], Ramona A. Zeno[1], Jarrod A. Santora[1,3]

[1]Farallon Institute for Advanced Ecosystem Research, Petaluma, California 94952, USA
[2]Department of Integrative Biology, University of California, Berkeley, California 94720, USA
[3]Center for Stock Assessment Research, University of California, Santa Cruz, California 95060, USA

ABSTRACT: In the California Current ecosystem, krill availability is a well-known influence on the demography of commercially and ecologically valuable fish, seabirds, and marine mammals. Modeling factors that enhance or inhibit krill aggregations, or 'hotspots', will benefit management of marine predators of conservation concern and contribute to ecosystem approaches to fisheries. Here, we link an oceanographic model (ROMS) and an individual-based model (IBM) parameterized for the krill species *Euphausia pacifica* to test the hypothesis that occurrences of krill hotspots are disassociated from centers of upwelling along the central-northern California coast due to strong advective currents that transport zooplankton away from the productive continental shelf environment. We compare the distribution of modeled to observed hotspots derived from hydroacoustic surveys from 2000 to 2008. Both acoustic data and modeled hotspots show the greater Gulf of the Farallones and Monterey Canyon as areas of persistent krill hotspots. In this large retention zone, we found no clear relationships between krill hotspots and proxies of upwelling. In contrast, modeled hotspots were associated with reduced upwelling (warmer sea surface temperature [SST] and lower alongshore currents) to the north of Pt. Reyes, and with enhanced upwelling (cooler SST and greater alongshore currents) south of Pt. Sur. Our model highlights the role spatial variability of physical forcing plays in determining the likelihood of krill hotspots forming in particular regions. Notably, our model reproduced the spatial organization of krill hotspots using only simple oceanographic forcing mechanisms and diurnal vertical migration behavior.

KEY WORDS: *Euphausia pacifica* · CCS · Offshore transport · Spatial prey structure · Upwelling

INTRODUCTION

Ecosystem modeling has become a standard tool in modern approaches to marine science, conservation, and management (Cury et al. 2008, Smith et al. 2011). In particular, the ecosystem approach to fisheries management as well as marine spatial planning requires accurate models which can be used to predict population processes, distributions, and ecological interactions in time and space (Link 2010). Ecological interactions include predator–prey relationships, which have been identified as important determinants of population and food web dynamics (Hunsicker et al. 2011). Recent research has focused on spatial ecology of food web dynamics, including the concept of spatial hotspots of trophic interactions where predator and prey interactions are concentrated (Sydeman et al. 2006, Hazen et al. 2013). To date, however, most studies of hotspots have been descriptive and empirical, focusing on locations of elevated predator abundance relative to physical conditions (e.g. Polovina et al. 2006 on loggerhead turtles, Yen et al. 2006 on seabirds), or less often, on the physics that may facilitate the distribution of

*Corresponding author: jdorman@faralloninstitute.org

predator–prey hotspots (Gende & Sigler 2006, Santora et al. 2011a). To our knowledge, no study has attempted to model prey hotspots in time and space.

The term 'hotspot' is often used to describe either locations of high biodiversity of species (Myers et al. 2000) or locations of higher local abundance of important species in the ecosystem (Dower & Brodeur 2004, Sydeman et al. 2006). These locations can range in spatial scale from 1 to 1000s of km. We use the term 'hotspot' to describe locations of prey aggregation in the coastal ocean, which can maximize the transfer of energy to higher trophic levels (Sydeman et al. 2006). We focus on aggregations on the mesoscale (10 to 100s of km) and on physical factors such as coastline/bathymetry (Nur et al. 2011, Wingfield et al. 2011) or wind-driven upwelling structure (Croll et al. 2005, Atwood et al. 2010) that may drive the spatial structure of these hotspots.

Prey hotspots in pelagic systems consist of species that constitute the forage nekton community (typically forage fishes, squids, and mesozooplankton). Euphausiid crustaceans ('krill') are key components of this community in many marine ecosystems, including the California Current (Field et al. 2006). While krill are abundant, they occur in distinct patches or hotspots of aggregation, and the distribution and spatial organization of krill prey patches is critically important to trophic interactions (Benoit-Bird et al. 2013). Krill are fed upon directly or indirectly by a diverse assemblage of meso- and top predators in the California Current, including seabirds (Ainley et al. 1996, Sydeman et al. 2006), marine mammals (Fiedler et al. 1998), and large predatory fishes (Reilly et al. 1992, Tanasichuk 1999, Lindley et al. 2009). For this reason, krill may be considered 'foundational species' (Dayton 1972) in epipelagic food webs.

Here, as an initial step towards understanding the mechanisms supporting krill hotspot dynamics in the California Current System (CCS) upwelling environment, we tested the hypothesis that the spatial distribution of krill hotspots is disassociated from centers of upwelling. Upwelling in the California Current is episodic in nature and the interplay between wind-driven upwelling events (importing nutrients to surface waters) and relaxation events with little wind (and therefore little associated advection of plankton to offshore waters) determines the productivity over the shelf region. This interplay is described by the 'optimal environmental window' hypothesis (Cury & Roy 1989), which predicts lower productivity under weak or intense upwelling and greatest productivity under moderate upwelling conditions. The negative impacts of intense advection have been modeled (Botsford et al. 2003, Dorman et al. 2011) and observed for krill (Santora et al. 2011a) in the California Current. To test this hypothesis we modeled krill hotspots over 9 yr, 2000 to 2008, using an oceanographic model coupled with an individual-based model (IBM; Dorman et al. 2011) designed for the dominant species in this ecosystem, *Euphausia pacifica* (Brinton & Townsend 2003). Initially, to verify model output on hotspots, we compared the distribution of modeled and observed krill aggregations. Subsequently, we investigated if proxies of upwelling (sea surface temperature [SST] and currents) in the model were positively or negatively associated with krill hotspots in different regions of our study area. This study is important as it represents a critical step towards understanding the distribution and dynamics of prey patches on synoptic time scales, the scale of dynamics that drive the foraging success and demographic responses of predators to variation in food resources.

MATERIALS AND METHODS

Regional Ocean Modeling System

The individual-based particle tracking model utilized ocean conditions from the Regional Ocean Modeling System (ROMS), a model commonly used to simulate the CCS (Powell et al. 2006, Di Lorenzo et al. 2008, Moore et al. 2011). ROMS was forced using a bulk-fluxes approximation (Fairall et al. 1996) with data from the National Centers for Environmental Prediction (NCEP) North American Regional Reanalysis (NARR) dataset (approximately 30 km resolution). Boundary and initial conditions were taken from the Simple Ocean Data Assimilation (SODA) model (Carton & Giese 2008) downloaded from the Asia-Pacific Data-Research Center (http://apdrc.soest.hawaii.edu). The modeled domain ranged from Newport, Oregon to Pt. Conception, California, and up to 1000 km offshore (Fig. 1). Model grid resolution was approximately 6 km in the alongshore and 3 km in the cross-shore direction. Average model output was saved daily.

Temperature in the coastal ocean simulated by ROMS correlated well with observed data collected at 8 buoys (National Data Buoy Center data), with correlation coefficients ranging from 0.6 to 0.7 ($p < 0.001$ at all stations; Fig. 2). Coastal currents also significantly correlated ($r = 0.6$ to 0.7 inshore; $r = 0.3$ to 0.5 offshore; $p < 0.001$ at all locations) with CODAR data collected by the Bodega Ocean Observing Network (Fig. 2).

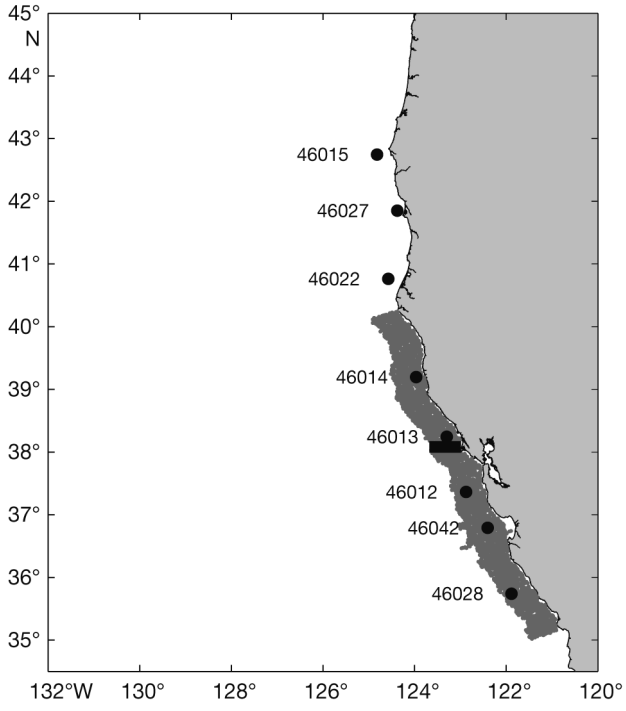

Fig. 1. Regional Ocean Modeling System (ROMS) model domain, individual-based model initial locations (grey, from 40° to 35° N along the coast), National Data Buoy Center (NDBC) stations utilized for temperature comparison (●), and Bodega Ocean Observing Network (BOON) CODAR data location (■ at ~38° N latitude)

Individual-based model

The IBM utilized was originally developed by Batchelder & Miller (1989) and has been previously used to model *Euphausia pacifica* population biology in the California Current (Dorman et al. 2011). Particle movements are implemented by interpolating currents spatially (from model grid points) and temporally (from saved ROMS model output) to the particle location, then integrated using a Runge-Kutta 4th-order advection scheme to update particle location. Vertical diffusivity is incorporated into vertical displacement though a diffusive random walk (Visser 1997) to avoid the accumulation of individuals in regions of low vertical diffusivity. Horizontal diffusivity is not implemented in particle tracking, as its impact on horizontal position is very small compared to horizontal current velocities. Diurnal vertical migration (DVM) is implemented using the methodology of Batchelder et al. (2002), with a maximum swimming speed of approximately 0.1 m s^{-1} (Torres & Childress 1983). In order to assess the physical impact of upwelling on hotspot formation, no biological parameterization (growth, life-stage development, reproduction, mortality) was implemented in this study.

We modeled the spring and summer of the years 2000 to 2008 using an ensemble approach where the upper limit of DVM was set at 5, 20, and 40 m (1 depth for each ensemble). Spring runs were designed to lead up to the time of our acoustic observations to look at hotspot formation, and summer runs were designed to see if modeled hotspots persisted beyond our acoustic observations. Variation in the DVM upper limit was utilized to examine the impact of vertical positioning on hotspot formation and cross-shelf location. The upper limit of DVM is highly variable in nature, resulting in a more diffuse population in the upper part of the water column, but prescribing set depths simplifies the interpretation of the data. A total of 54 realizations of the IBM were computed for this study. All model runs started with identical initial conditions and ran for 90 d from the starting date. The 'spring' runs (n = 27, 3 ensembles) began on February 15 of the years 2000 to 2008, and 'summer' runs (n = 27, 3 ensembles) used May 15 as the starting date. The model data are at a higher resolution, both temporally and spatially (90 continuous days over the entire domain), than the data collected via hydroacoustics. To determine if such dense model data had an impact on our results, analyses using all the data were compared to randomly subsampled model data. No significant differences were detected in the results, except for the influence of initial conditions. For that reason, model days 1 to 30 are not used in the analyses.

Hydroacoustic data

Estimates of krill hotspot distribution were made based on hydroacoustic surveys conducted in May and June each year by the NOAA-National Marine Fisheries Service over the coastal ocean of the central-northern California shelf (Sakuma et al. 2006; Fig. 3a). The focus of our analysis was on the survey effort from 2000 to 2008 (except 2007, when no acoustic data were available), and data collected between Pt. Sur (36.6° N, 121.9° W) and Pt. Arena (39.0° N, 123.7° W). Ships used in this study (usually the RV 'David Starr Jordon') were equipped with echosounders, which ran continuously throughout the survey period (multi-frequency SIMRAD EK500 or EK60) and were used to estimate the volume of micronekton in the water column. Krill was distinguished from other backscattering signals using a 3-frequency ΔS_v method (Hewitt & Demer 2000, Watkins & Brierley 2002). The nautical

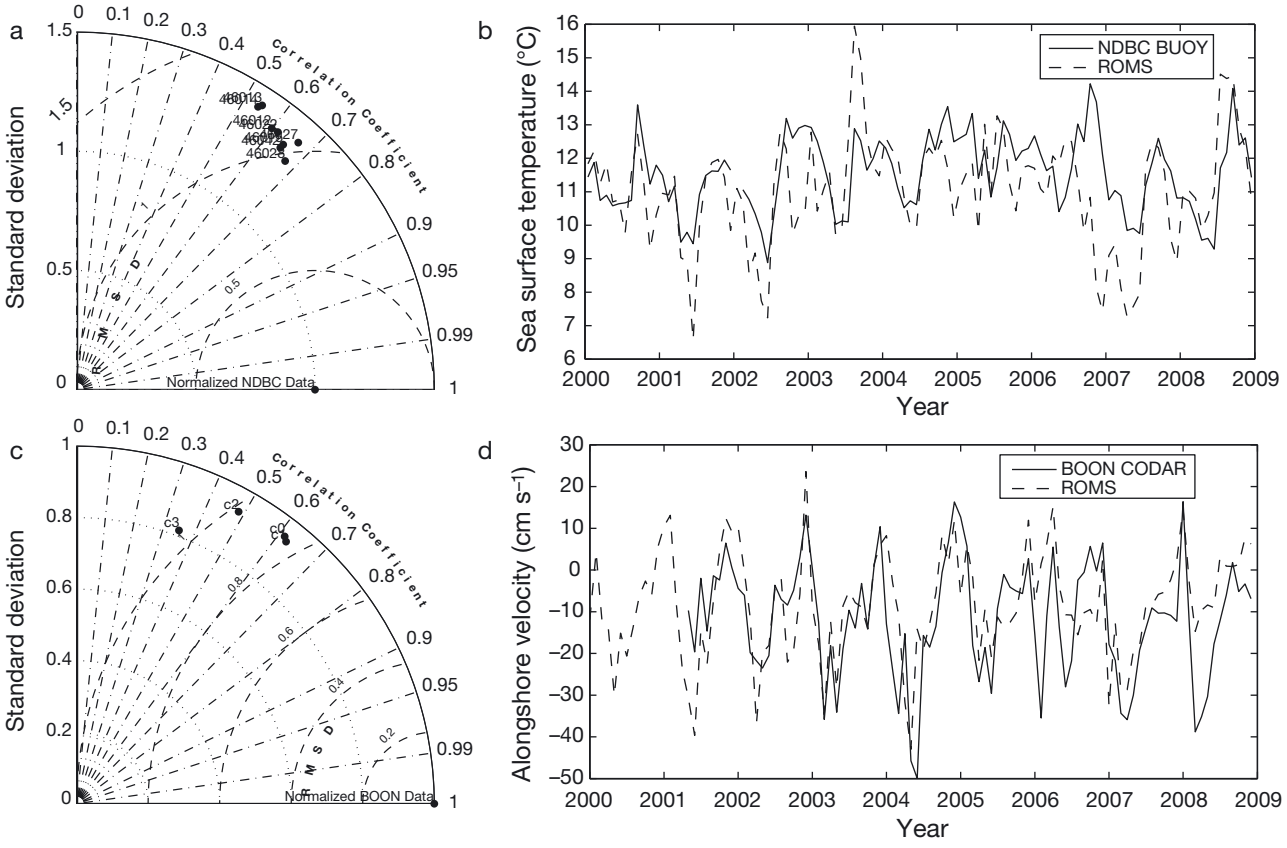

Fig. 2. (a,c) Taylor diagrams and (b,d) time-series of observed and modeled (a,b) sea surface temperature and (c,d) alongshore surface currents (positive: northward; negative: southward). Taylor diagrams display correlation coefficient (curved exterior axis), normalized standard deviation, and root mean squared deviation (RMSD, curved interior axis). Station locations correspond to (a) NDBC Station IDs and (c) CODAR regions from onshore (c0) to offshore (c3) identified in Fig. 1. Time-series are from NDBC Buoy 46013 (temperature) and the most inshore CODAR region (alongshore surface currents). Solid lines: observations; dashed lines: the ROMS model

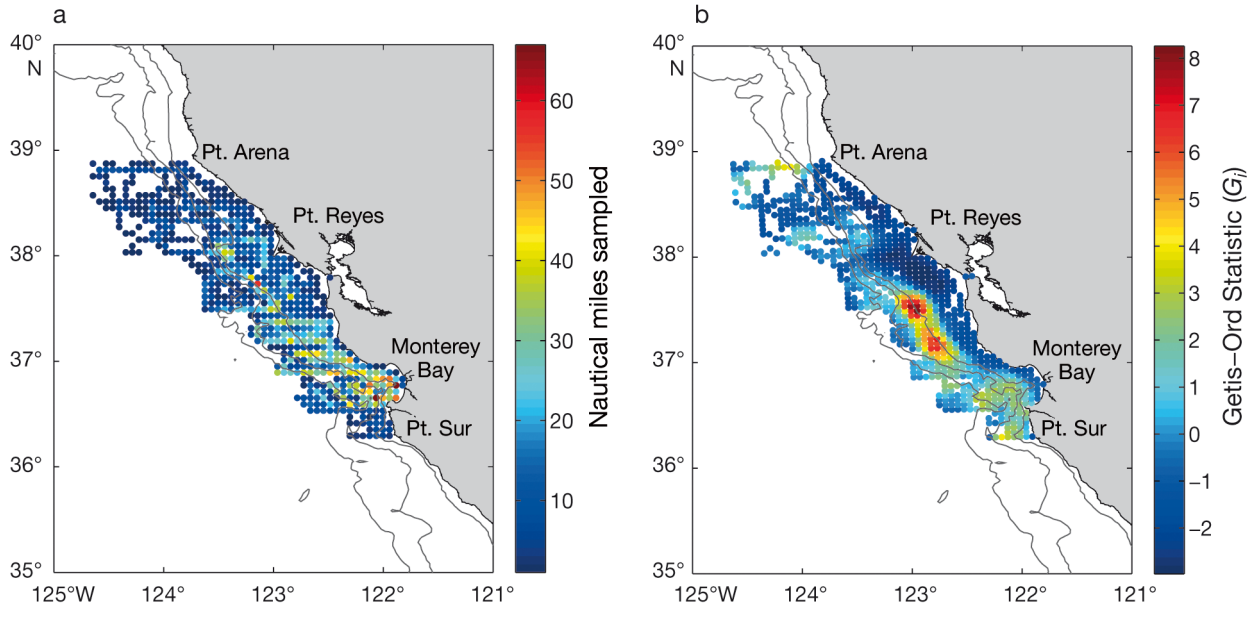

Fig. 3. (a) Acoustic sampling effort and (b) acoustic clustering analysis (Getis-Ord statistic) from 2000 to 2008. Isobaths included are 200, 1000, and 2000 m

acoustic scattering coefficient (NASC, m^2 nautical mile $[nmi]^{-1}$) is a depth-integrated index of horizontal krill distribution and abundance (Simmonds & MacLennan 2005). NASC values were integrated vertically, from 250 m depth to 10 m from the surface, and horizontally into 1 nmi increments associated at the midpoint with latitude and longitude. Echograms were visually examined using Echoview 4.9 (Myriax) to ensure no bottom or surface contamination affected integrated NASC values. This effort and the resulting NASC data set are similar to those obtained during NOAA Juvenile Rockfish Surveys in previous years (Santora et al. 2011a). Krill distributions for the entire survey domain were compiled into discrete 25 km^2 grid cells (Santora et al. 2011a). This cell size was chosen to minimize effects of spatial autocorrelation (Fortin 1999, Dungan et al. 2002). Average NASC by cell for the years 2000 to 2008 was calculated in ArcMap™10 (ESRI).

Analysis

We first determined the spatial coherence between observed and modeled krill hotspots. To accomplish this we employed the Getis-Ord statistic (G_i; Getis & Ord 1992) to quantify and map hotspots based on acoustic krill observations (grid-averaged spatial means for May and June) and modeled concentrations of particle densities (clusters of particles per daily time step). G_i is a statistical measurement (a Z-score) of local clustering (spatial intensity) relative to the background spatial mean and standard deviation (see Santora et al. 2010 for an application). A spatial neighborhood was set as 42 km alongshore and 15 km across-shore; these criteria were selected based on Moran's I tests of spatial autocorrelation in the acoustic data (Santora et al. 2011a). Significant G_i values that were spatially contiguous were grouped into hotspots. For modeled data, where multiple days of observations are available for each year, the number of days of significant and positive G_i values was tallied for each model run, and the average number of significant days was computed from the 9 yr of model data.

Secondly, we quantified relationships between modeled krill hotspots and underlying habitat characteristics. Specifically, we sought to describe the relationships between modeled krill hotspots and hydrographic conditions of the northern (>38° N, north of Pt. Reyes), central (between 38° and 36° N), and southern (<36° N, south of Pt. Sur) regions, and by season, spring and summer. We used nonparametric generalized additive models (GAM) to quantify relationships between the daily intensity of modeled krill hotspots and corresponding hydrographic conditions focusing on temperature and currents obtained from ROMS (similar to Santora et al. 2012). The fitted GAMs for modeled krill hotspots (dependent variable is G_i intensity; Z-score was normally distributed) was specified with a Gaussian distribution and an identity-link function. GAMs were implemented using the 'mgcv' package in the R statistical program (R Development Core Team 2013); smoothness parameters (s) were estimated with generalized cross-validation (Wood 2006). Adjusted R^2 and percent deviance explained were obtained to evaluate model performance. By default, the G_i statistic for each identified modeled hotspot collectively represents a scaling of the intensity of particle clustering within each hotspot; some hotspots exhibit higher spatial intensity than others. The effect of each covariate included in the GAM was plotted to visually inspect the functional form (e.g. linear or non-linear smoothed fit) to permit description of threshold responses of modeled krill hotspots to changes in ocean conditions.

A priori, we knew that observed krill hotspots (May and June) exhibit a non-uniform spatial clustering pattern along the California coast (variation by latitude), with hotspots localized in the Gulf of the Farallones and generally downstream from strong upwelling zones (Santora et al. 2011a). Our first GAM therefore compared the average intensity of each modeled hotspot location (from both spring and summer runs and each DVM ensemble) to latitude to ascertain if this spatial pattern was reproduced by the particle tracking model; GAM_1: $G_i \sim s$(latitude). Secondly, we compared the daily G_i value of each hotspot to daily physical data from the ROMS model to analyze their influence on hotspot formation (i.e. clustering of 'krill particles'). SST and meridional (north/south) surface flow (V-current) around the selected hotspot were analyzed for each set of model runs (spring and summer); GAM_2: $G_i \sim s$(SST) + s(V-current).

RESULTS

Observed krill hotspots

Analysis of acoustic data with the Getis-Ord statistic (G_i) identified 3 areas of significant hotspots that ranged from 313 to 1113 km^2 in size with 5 peaks in G_i values (Table 1, Fig. 3b). Distance of peak G_i to the coast ranged from 20.3 to 58.9 km. All observed hotspots were found offshore of the 200 m isobath. The hotspot off of Pt. Arena (Table 1, Hotspot A1)

falls along the 2000 m isobath on Arena Canyon. The most intense area of clustering occurred along the San Mateo coastline from San Francisco Bay to Año Nuevo Canyon (Table 1, Hotspots A2 and A3) and contained 2 peaks in intensity. Hotspot A2 is located on the northern boundary of the Monterey Bay National Marine Sanctuary (37.5° N, 122.9° W) just offshore of the 200 m isobath. Hotspot A3 is more southerly (37.2° N, 122.7° W) and is also located just offshore of the 200 m isobath. The most southerly area of clustering is offshore of Monterrey Bay and Pt. Sur and also contains 2 peaks in intensity (Table 1, Hotspots A4 and A5). Hotspot A4 falls along the Monterey Canyon (36.6° N, 122.3° W) and is located 58.9 km offshore of Moss Landing. Hotspot A5 is 20.3 km offshore from Pt. Sur, saddled between the 200 and 1000 m isobaths.

Modeled krill hotspots

Each ensemble of runs (e.g. all years: 2000 to 2008 for the start date February 15, and upper limit of DVM = 5 m) identified 5 to 10 hotspots, with a total of 44 hotspots found over the 6 sets of runs. When the upper limit of DVM was set at 5 m, the average distance of modeled hotspots was further offshore (37.6 ± 13.1 km, mean ± standard deviation) than when set at 20 m (20.0 ± 3.2 km) or 40 m (18.1 ± 6.9 km) (Figs. 4 & 5). Modeled hotspots were consistently found along the San Mateo coastline and above Monterey Canyon for all sets of models run (spring or summer, and all upper limits of DVM; Table 1). The San Mateo hotspot (M1) was very consistent and was present 57% of the model run time with an average size of 925 km^2. The Monterey Canyon hotspot (M2) was present 25% of the time with an average size of 660 km^2. The intensity of these 2 hotspot locations and the intensity of all other identified hotspots in Fig. 5 were examined with respect to physical factors.

Environmental determinants of modeled hotspots

GAMs revealed the relationship between the spatial intensity of modeled krill hotspots and hydrographic variability (Table 2, Figs. 6 & 7). A non-linear parabolic relationship was identified between average G_i and latitude of modeled hotspots (GAM_1; Fig. 6), confirming clustering of hotspots between Pt. Reyes and Pt. Sur in the greater Gulf of the Farallones. GAM_2 revealed contrasting functional relationships between the spatial intensity of modeled hotspots and SST and V-currents within each region (Table 2, Fig. 7); results were similar between spring and summer (Fig. 7 shows only spring data). Notably, the relationship between modeled hotspots and SST and V-current in the northern region was contrary to that in the southern region (Fig. 7). In the northern region, relationships were generally linear with increasing intensity of modeled hotspots associated with warmer SST (>9°C) and weaker southerly currents (Fig. 7a,b), both proxies of relaxed upwelling (or downwelling) conditions. In the central region, the relationship between modeled hotspot intensity and SST was complex and not clear (Fig. 7c), but hotspots were more intense when V-currents were

Table 1. Summary of significant krill *Euphausia pacifica* hotspots from acoustic surveys and model runs from May and June 2000 to 2008. Distance to feature (isobaths, coast) in km; signs in parentheses indicate inshore (–) and offshore (+); ref. land point is reference to nearest land on Californian coast or island

Hotspot (ID)	G_i	Location of peak G_i	Area (km^2)	Distance to feature (km)		
				200 m	1000 m	Coast (ref. land point)
Acoustic						
Pt. Arena (A1)	3.93	38.8° N, 124.1° W	312.5	18 (+)	7 (+)	33.9 (Pt. Arena)
SE Farallones (A2)	8.26	37.5° N, 122.9° W	862.5	0.43 (+)	12.3 (–)	22.9 (SE Farallones)
Pescadero (A3)	6.88	37.2° N, 122.7° W	1112.5	0.61 (+)	19.4 (–)	33.5 (Pescadero)
Moss Landing (A4)	3.15	36.6° N, 122.3° W	912.5	33.4 (+)	15.4 (+)	58.9 (Moss Landing)
Pt. Sur (A5)	3.13	36.3° N, 122.1° W	162.5	9.9 (+)	9.6 (–)	20.3 (Pt. Sur)
Modeled						
Hotspot (ID)	%Time hot	Location of peak value	Area (km^2)	Distance to feature (km)		
				200 m	1000 m	Coast (ref. land point)
San Mateo (M1)	56.7	37.3° N, 122.6° W	925	18.5 (–)	34.6 (–)	19.9 (Pescadero)
Monterey Canyon (M2)	24.9	36.7° N, 122.2° W	660	14.5 (+)	0.1 (+)	66.5 (Moss Landing)

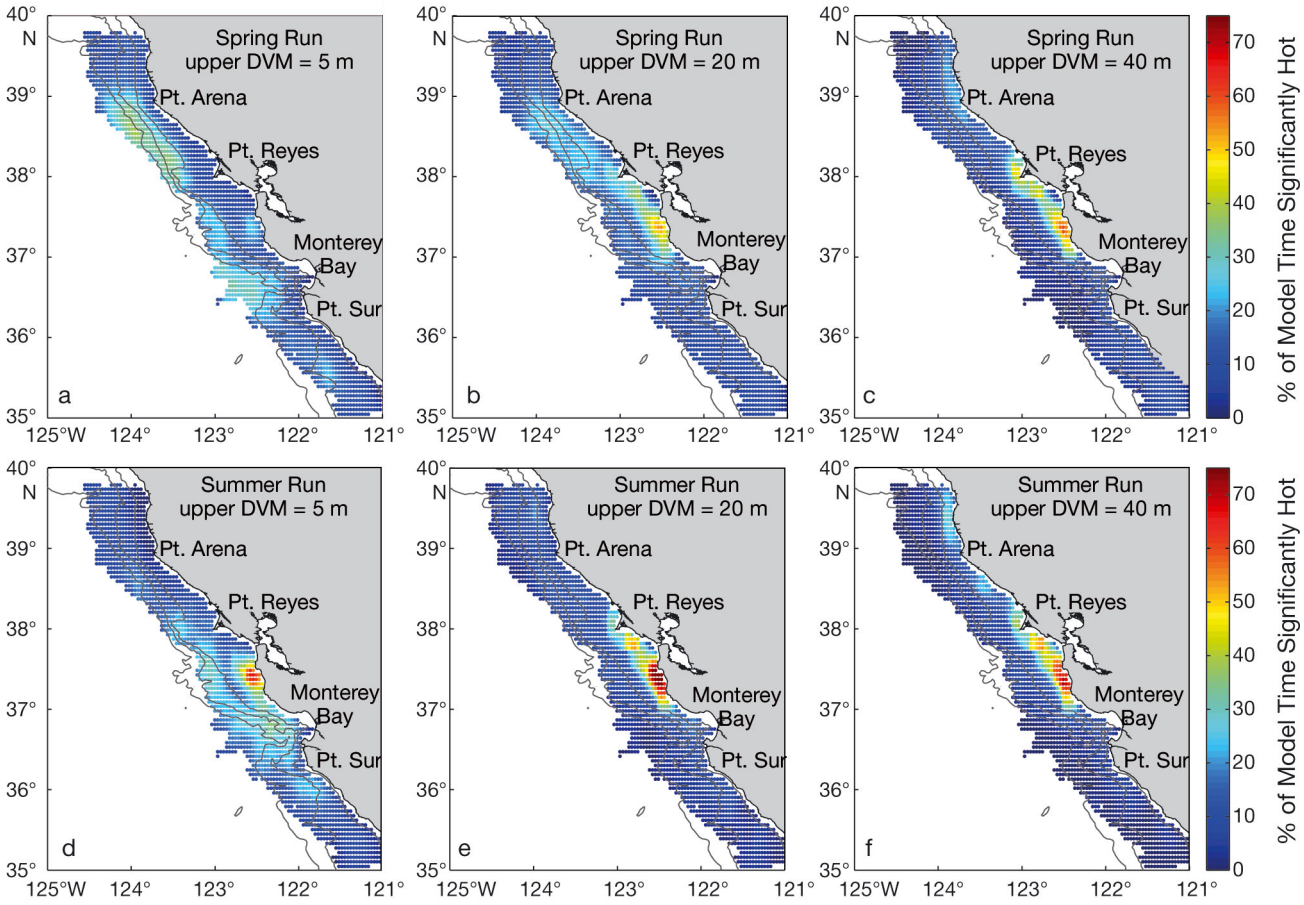

Fig. 4. Percentage of model run time that the coastal region was significantly clustered (hot). (a–c) Spring runs and (d–f) summer runs with an upper limit of diurnal vertical migration (DVM) at (a,d) 5 m, (b,e) 20 m, and (c,f) 40 m. Isobaths included are 200, 1000, and 2000 m

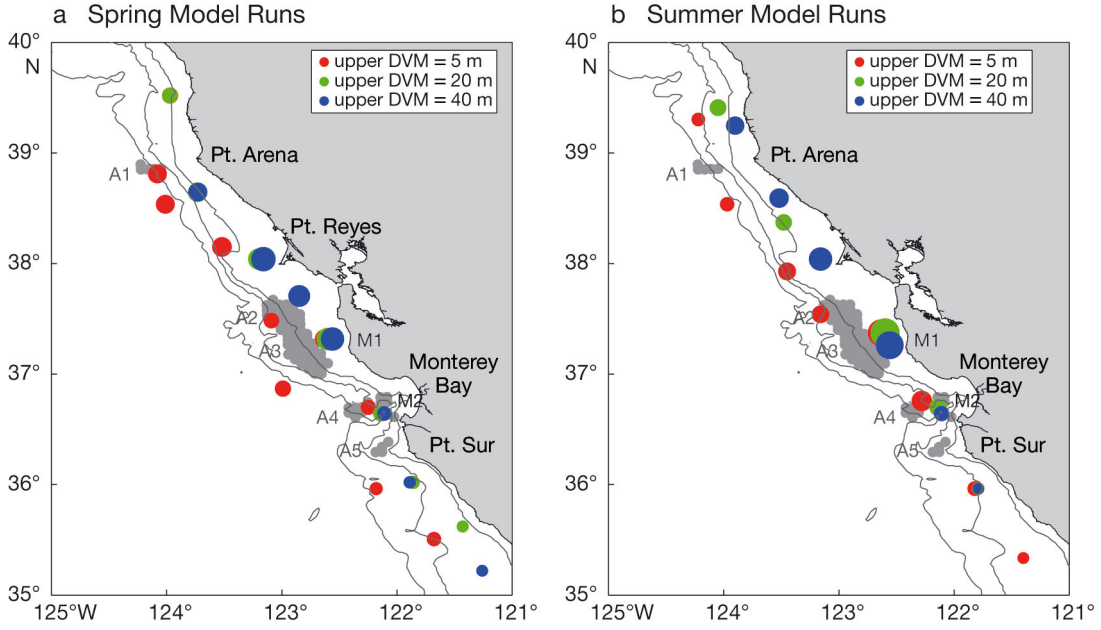

Fig. 5. Hotspots identified from (a) spring and (b) summer model runs. Size of marker identifies the number of days the location was identified as a significant hotspot ranging from a maximum of 45 d (largest marker) to a minimum of 10 d (smallest marker). Grey patches are hotspots ($p < 0.01$) identified from the acoustic data. The acoustic (A1 to A5) and modeled (M1 and M2) hotspots from Table 1 are indicated. Isobaths included are 200, 1000, and 2000 m

Table 2. Results of generalized additive models for comparing modeled hotspot intensity to ocean surface conditions (sea-surface temperature [SST] and daily meridional surface currents [V-current] within sub-regions of the Californian coast. edf: estimated degrees of freedom; Ref.df: estimated residual degrees of freedom; gcv: generalized cross-validation score

Covariate	North					Central					South				
	edf	Ref.df	*F*	p	R^2	gcv	edf	Ref.df	*F*	p	R^2	gcv	edf	Ref.df	*F*	p	R^2	gcv
Spring																		
SST	5.94	7.14	36.54	<0.0001	0.27	4.72	8.5	8.94	52.60	<0.00001	0.24	8.02	7.31	8.31	31.92	<0.0001	0.35	3.28
V-current	5.49	6.71	8.34	<0.0001			5.4	6.54	17.15	<0.00001			3.93	4.93	2.81	0.017		
Summer																		
SST	8.74	8.98	32.94	<0.0001	0.24	4.82	8.2	8.83	67.26	<0.0001	0.39	7.54	1.68	2.11	49.73	<0.0001	0.19	1.45
V-current	5.22	6.39	9.73	<0.0001			7.8	8.64	9.29	<0.0001			3.56	4.49	5.11	<0.0001		

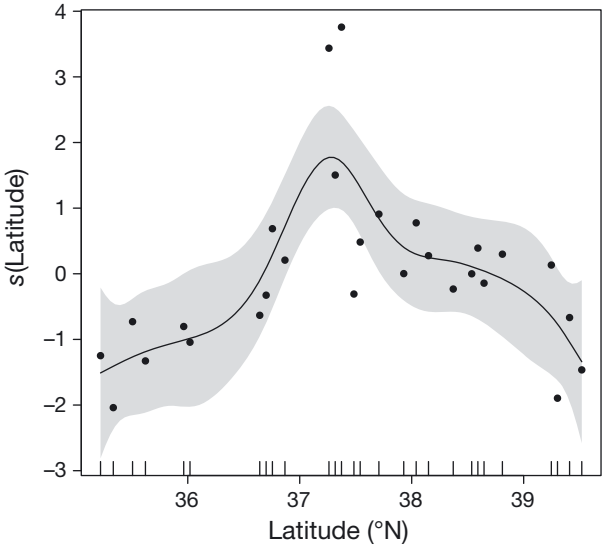

Fig. 6. Results of generalized additive model for evaluating the functional relationship between latitude and average Getis-Ord value at each modeled krill *Euphausia pacifica* hotspot. Shaded grey area represents 95% CI and tick marks represent data availability

more southerly (Fig. 7d). In the southern region, the relationship between modeled hotspot intensity and SST or V-current was negative, suggesting that hotspots were more likely to form during periods of upwelling (cooler SST and increased southerly flow; Fig. 7e,f).

DISCUSSION

In this study, we modeled krill aggregations to test the hypothesis that krill hotspots are disassociated from regions of more intense upwelling and greater Ekman transport. Our model consistently formed hotspots that were similar in size, location, and intensity to acoustically observed krill hotspots (Santora et al. 2013), albeit with a small longitudinal offset. Our model runs aimed to simulate hotspots in different seasons (spring and summer) and based on different vertical migration schemes (upper limit of 5, 20, or 40 m). We found similar results during spring and summer model runs, but found that variation in the upper limit of DVM impacted the spatial distribution of our modeled prey fields. Modeled hotspots were consistently located further offshore when the upper limit of vertical migration was 5 versus 20 or 40 m, as surface currents in a coastal upwelling environment like the California Current are more likely to be moving offshore. These results agree with observations of the cross-shelf location of zooplankton populations

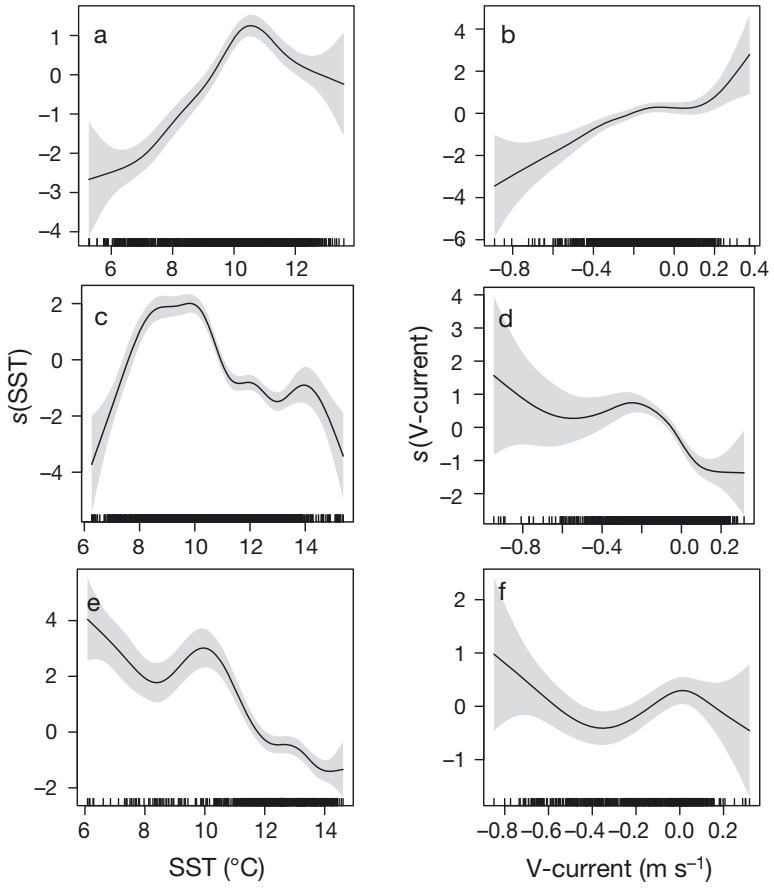

Fig. 7. Results of generalized additive model for evaluating the functional relationship between daily sea-surface temperature (SST), daily meri dional surface currents (V-current) and daily Getis-Ord value at modeled krill *Euphausia pacifica* hotspots from the spring suite of runs. Results are from (a,b) north of 38° N, (c,d) between 38° and 36° N and (e,f) south of 36° N. Shaded grey area represents 95% CI and tick marks represent data availability

under variable states of upwelling (Papastephanou et al. 2006).

Prescribing a static depth to the upper limit of DVM is instructive in diagnosing the impact of a specific behavior, but is not a true representation of *Euphausia pacifica* vertical migration behavior. Field observations (acoustic and depth stratified net hauls) often show greater variability in the vertical distribution of the population at night (Endo & Yamano 2006). As the objective of ascending during vertical migration is to feed in productive surface waters (Forward 1988), variability in the depth of the surface food resources, searching behavior to find food sources, or sufficient food resources at depth can all impact the upper extent of vertical distribution. Considering this, the hotspot locations of any one ensemble of model runs (5 vs. 20 vs. 40 m) might not be indicative of hotspots of the entire population, but taken together they represent the spectrum of actual vertical migration behavior. We emphasize the importance of the model hotspots identified in Table 1 (Hotspots M1 and M2), as they were realized under all 3 vertical migration schemes.

Comparison of observed and modeled hotspots

The analysis of acoustic data (observations) with the Getis-Ord statistic identifies 3 locations that were significantly more clustered than the rest of the sampled area over the years 2000 to 2008. These findings are similar to previous results derived using kernel density smoothing procedures (Santora et al. 2011a). The largest of these observed acoustic hotspots were between Pt. Reyes and Pt. Sur, one located off the San Mateo coastline (Hotspots A2 and A3) and one associated with Monterey Canyon (Hotspot A4). Our modeling efforts identified hotspots throughout the domain, but these same 2 locations were (1) significantly more 'hot' than other locations, and (2) were identified as hotspots regardless of the vertical migration scheme employed. In addition, they were found in similar locations and at fairly similar sizes as the observed hotspots from the acoustic data. The agreement between observed acoustic data and the model (under all 3 DVM scenarios) gives us confidence in the model results and highlights the importance of these locations.

These 2 identified hotspots agree with other non-acoustic field data that identify them as important foraging sites for krill predators. The area south of Pt. Reyes that encompasses Hotspots M1, A2, and A3 (Table 1) is a region of increased chlorophyll *a* (Vander Woude et al. 2006, Suryan et al. 2012). We did not model krill growth as part of our model runs, but the co-occurrence of phytoplankton, a primary food source of *E. pacifica* (Ohman 1984), and our *E. pacifica* individuals is not surprising in light of both organisms' planktonic nature. Increased phytoplankton abundance in these regions has the potential to further enhance krill hotspots via increased reproductive output or increase predator feeding efficiency through larger, more energetic, individual

krill. This region is also a critical foraging habitat for juvenile salmon as they enter the ocean (Lindley et al. 2009) and for a multitude of seabirds that nest on the Farallon Islands (Sydeman et al. 2006, Mills et al. 2007). Monterey Canyon is a location that supports dense aggregations of krill (Marinovic et al. 2002, Croll et al. 2005, Santora et al. 2011a), and is also a well-known foraging location for seabirds (Yen et al. 2004, Santora et al. 2011b) and marine mammals (Yen et al. 2004, Croll et al. 2005). The aggregation of krill in these regions further enhances the feeding efficiency of top predators (Goldbogen et al. 2011) of the central California Current.

Due to the importance of krill to the entire ecosystem and the stated goal of the Pacific Fisheries Management Council to manage resources with ecosystem considerations in mind, there is currently a prohibition on the harvest of krill in US waters of the California Current. Coastal waters out to the 1000 fathom (1829 m) depth contour have been designated as Essential Fish Habitat for the species and the specific locations of our hotspots were considered, but not designated, as Habitat Areas of Particular Concern (HAPC) (Southwest Fisheries Science Center 2008). Should a fishery for krill ever be opened, these hotspot locations should be designated as HAPC where krill harvest would be prohibited.

Environmental determinants of modeled hotspots

Our modeled hotspots appear to show a distinct response to upwelling, generally becoming less intense, or disappearing entirely under intense upwelling conditions. We recognize that the physical variables we compare with hotspot formation, SST and alongshore currents, are not the actual physical processes responsible for generating hotspots, but are proxies for the ensemble of processes that produce hotspots (discussed below). These processes operate over time and space and their integrated effects influence when and where hotspots might form. This discrepancy may explain some of the differences we see in certain regions and why we only observe hotspot at intermediate levels of SST and current velocities.

Our model results show a distinct difference in the average intensity of modeled hotspots across the latitudinal gradient of our domain (Fig. 6). While we found hotspots throughout the domain, regions to the north of Pt. Reyes and the south of Pt. Sur contained fewer and less intense hotspots. Santora et al. (2011a) hypothesized that decreases in acoustic krill abundance were related to increased Ekman transport, and our results generally support this theory throughout the domain, most strongly to the north of Pt. Reyes on a stretch of coastline known for intense upwelling (Largier et al. 2006). GAM results show that 2 indicators of upwelling (cold SST and negative V-current) are negatively related to hotspot formation to the north of Pt. Reyes. These results support the optimal environmental window hypothesis (Cury & Roy 1989, Botsford et al. 2003), and indicate that high intensity upwelling, and the strong advective currents that characterize the nearshore environment, can disrupt hotspot formation along this stretch of coastline. The data further indicate that more intense upwelling conditions (V-current less than -0.4 m s^{-1}, Fig. 7b) inhibit hotspot formation. Under weaker or non-upwelling conditions (V-current between -0.4 and 0.2 m s^{-1}), the model may or may not produce hotspots, indicating that 'adequate' physical conditions do not guarantee the presence of krill particles and the formation of a hotspot.

GAM results show that hotspot formation to the south of Pt. Reyes and to the north of Pt. Sur (in the Gulf of the Farallones) occurs more often during upwelling-favorable conditions (colder temperatures and southerly alongshore flow). Both the acoustic and model data identified this stretch of coastline as having the most intense and persistent krill aggregations. Latitudinal variability in forcing and local bathymetric features may play a role in retaining krill in this region. In general, the intensity of upwelling-favorable winds in the Gulf of the Farallones is weaker than to north of Pt. Reyes (García-Reyes & Largier 2012). Our modeled oceanographic conditions agree, as the region is both warmer and meridional currents are weaker compared with data from north of Pt. Reyes. Thus the high intensity upwelling that inhibits hotspots to the north is not apparently an issue for krill in the central region. Coastal retention can be inhibited by more narrow continental shelves (Botsford et al. 2006) and thus retention may be enhanced in the Gulf of the Farallones region, relative to the north of Pt. Reyes, by the wider continental shelf which requires stronger and more persistent surface currents to advect particles off the shelf to oceanic waters. The krill aggregations over Monterey Canyon (Hotspots A4 and M2) may also persist due to the canyon bathymetry which enhances retention (Allen et al. 2001). Finally, both of the major hotspots identified in the model are to the south of the Pt. Reyes headland. This headland directs the strong alongshore currents from the north offshore (Strub et al. 1991) and creates an 'upwelling shadow'

to the south (Wing et al. 1998, Largier 2004, Vander Woude et al. 2006). While the San Mateo hotspot (Hotspot M1) is slightly to the south of the area typically defined as the Pt. Reyes upwelling shadow, the upwelling shadow may exert some influence on local aggregations via protection from strong currents or as a source of particles supplying the downstream San Mateo hotspot.

To the south of Pt. Sur, the relationship between modeled hotspots and ocean conditions is not as clear as it is to the north. The GAM results concerning V-current are the least significant of all measured; indeed, alongshore currents do not appear to influence hotspot intensity in any meaningful manner. The significant relationship between hotspot intensity and cooler SSTs suggests that hotspots generally form during upwelling-favorable conditions. Yet, SST often remains warm during upwelling events in the region (García-Reyes & Largier 2012) due to greater stratification and upwelling of warmer water from above the pycnocline. It should also be noted that identified hotspots to the south of Pt. Sur are some of the least persistent identified by the models, present less than 15% of the modeled run time.

Model limitations

There are other physical and biological factors that could influence hotspot intensity that are not included in our model. These include reproductive dynamics, horizontal swimming behavior of *E. pacifica*, or spatial variability in predation pressures. Little is known about swimming behavior in *E. pacifica* other than vertical migration behavior and predatory escape responses. While krill are considered planktonic, their strong swimming ability puts them at the boundary of plankton/nekton and it is conceivable that they might incorporate horizontal swimming to maintain position or aggregate near small-scale food resources. Also, little is known about differences in spatial patterns of predation of krill in the California Current. While these biological factors certainly impact krill abundance and distribution, their impacts are beyond the scope of this modeling effort.

CONCLUSIONS

We reproduced acoustically observed krill hotspots using a coupled ROMS-IBM model, with only simple physical forcing and vertical migration behavior. This indicates the importance of transport in the formation of key biological aggregations of potential prey in the California Current. Collection and analysis of acoustic data provides us with a static view of hotspots during a given sampling period, whereas our model allows us to observe these hotspots under varying environmental conditions. This provides information on drivers of hotspot intensity, and suggests that hotspot formation is most likely under intermediate/moderate levels of upwelling. We showed that hotspots are found throughout our domain, but are most intense (and persistent) along the San Mateo coastline in the Gulf of the Farallones and over Monterey Canyon. Modeled hotspots tended to be more ephemeral to the north of Pt. Reyes and to the south of Pt. Sur. Understanding how physical factors drive spatial dynamics is of importance due to the impact of prey clustering on feeding efficiency of predators in the California Current.

Acknowledgements. We gratefully thank the many communities that provide data to make a modeling project such as this possible: National Centers for Environmental Prediction, Asia-Pacific Data Research Center, National Oceanographic Data Center, NOAA-National Data Buoy Center, Bodega Ocean Observing Node, NASA-Goddard Space Flight Center. Model development by the ROMS community and by Dr. Hal Batchelder have also been instrumental in this work. We are grateful for the extensive acoustic data collected by the National Marine Fisheries Service that contributed to model validation in this study. This research was supported by California Sea Grant Project R/ENV-220.

LITERATURE CITED

Ainley DG, Spear LB, Allen SG (1996) Variation in the diet of Cassin's auklet reveals spatial, seasonal, and decadal occurrence patterns of euphausiids off California, USA. Mar Ecol Prog Ser 137:1–10

Allen SE, Vindeirinho C, Thomson RE, Foreman MGG, Mackas DL (2001) Physical and biological processes over a submarine canyon during an upwelling event. Can J Fish Aquat Sci 58:671–684

Atwood E, Duffy-Anderson JT, Horne JK, Ladd C (2010) Influence of mesoscale eddies on the icthyoplankton assemblages in the Gulf of Alaska. Fish Oceanogr 19: 493–507

Batchelder HP, Miller CB (1989) Life history and population dynamics of *Metridia pacifica*: results from simulation modeling. Ecol Model 48:113–136

Batchelder HP, Edwards CA, Powell TM (2002) Individual based models of copepod populations in coastal upwelling regions: implications of physiologically and environmentally influenced diel vertical migration on demographic success and nearshore retention. Prog Oceanogr 53:307–333

Benoit-Bird KJ, Battaile BC, Heppell SA, Hoover B and others (2013) Prey patch patterns predict habitat use by top marine predators with diverse foraging strategies. PLoS ONE 8:e53348

Botsford LW, Lawrence CA, Dever EP, Hastings A, Largier J (2003) Wind strength and biological productivity in upwelling systems: an idealized study. Fish Oceanogr 12: 245–259

Botsford LW, Lawrence CA, Dever EP, Hastings A, Largier J (2006) Effects of variable winds on biological productivity on continental shelves in coastal upwelling systems. Deep-Sea Res II 53:3116–3140

Brinton E, Townsend A (2003) Decadal variability in abundances of the dominant euphausiid species in the southern sectors of the California Current. Deep-Sea Res II 50: 2449–2472

Carton JA, Giese BS (2008) A reanalysis of ocean climate using Simple Ocean Data Assimilation (SODA). Mon Weather Rev 136:2999–3017

Croll DA, Marinovic B, Benson S, Chavez FP, Black N, Ternullo R, Tershy BR (2005) From wind to whales: trophic links in a coastal upwelling system. Mar Ecol Prog Ser 289:117–130

Cury P, Roy C (1989) Optimal environmental window and pelagic fish recruitment success in upwelling areas. Can J Fish Aquat Sci 46:670–680

Cury PM, Shin YJ, Planque B, Durant JM and others (2008) Ecosystem oceanography for global change in fisheries. Trends Ecol Evol 23:338–346

Dayton PK (1972) Toward an understanding of community resilience and the potential effects of enrichments to the benthos at McMurdo Sound, Antarctica. In: Parker BC (ed) Proceedings of the Colloquium on Conservation Problems in Antarctica. Allen Press, Lawrence, KS, p 81–96

Di Lorenzo E, Schneider N, Cobb KM, Franks PJS and others (2008) North Pacific Gyre Oscillation links ocean climate and ecosystem change. Geophys Res Lett 35: L08607, doi:10.1029/2007GL032838

Dorman JG, Powell TM, Sydeman WJ, Bograd SJ (2011) Advection and starvation cause krill (*Euphausia pacifica*) decreases in 2005 Northern California coastal populations: implications from a model study. Geophys Res Lett 38:L04605, doi:10.1029/2010GL046245

Dower JF, Brodeur RD (2004) The role of biophysical coupling in concentrating marine organisms around shallow topographies. J Mar Syst 50:1–2

Dungan JL, Perry JN, Dale MRT, Legendre P and others (2002) A balanced view of scale in spatial statistical analysis. Ecography 25:626–640

Endo Y, Yamano F (2006) Diel vertical migration of *Euphausia pacifica* (Crustacea Euphausiacea) in relation to molt and reproductive processes, and feeding activity. J Oceanogr 62:693–703

Fairall CW, Bradley EF, Rogers DP, Edson JB, Young GS (1996) Bulk parameterization of air–sea fluxes for Tropical Ocean–Global Atmosphere Coupled–Ocean Atmosphere Response Experiment. J Geophys Res 101: 3747–3764

Fiedler PC, Reilly SB, Hewitt RP, Demer D and others (1998) Blue whale habitat and prey in the California Channel Islands. Deep-Sea Res II 45:1781–1801

Field JC, Francis RC, Aydin K (2006) Top-down modeling and bottom-up dynamics: Linking a fisheries-based ecosystem model with climate hypotheses in the northern California Current. Prog Oceanogr 68:238–270

Fortin MJ (1999) Effects of quadrat size and data measurement on the detection of boundaries. J Veg Sci 10:43–50

Forward RB (1988) Diel vertical migration — zooplankton photobiology and behavior. Oceanogr Mar Biol Annu Rev 26:361–393

García-Reyes M, Largier JL (2012) Seasonality of coastal upwelling off central and northern California: new insights, including temporal and spatial variability. J Geophys Res 117:C03028, doi:10.1029/2011JC007629

Gende SM, Sigler MF (2006) Persistence of forage fish 'hot spots' and its association with foraging Steller sea lions (*Eumetopias jubatus*) in southeast Alaska. Deep-Sea Res II 53:432–441

Getis A, Ord JK (1992) The analysis of spatial association by use of distance statistics. Geogr Anal 24:189–206

Goldbogen JA, Calambokidis J, Oleson E, Potvin J, Pyenson ND, Schorr G, Shadwick RE (2011) Mechanics, hydrodynamics and energetics of blue whale lunge feeding: efficiency dependence on krill density. J Exp Biol 214: 131–146

Hazen EL, Suryan RM, Santora JA, Bograd SJ, Watanuki Y, Wilson RP (2013) Scales and mechanisms of marine hotspot formation. Mar Ecol Prog Ser 487:177–183

Hewitt RP, Demer DA (2000) The use of acoustic sampling to estimate the dispersion and abundance of euphausiids, with an emphasis on Antarctic krill, *Euphausia superba*. Fish Res 47:215–229

Hunsicker ME, Ciannelli L, Bailey KM, Buckel JA and others (2011) Functional responses and scaling in predator-prey interactions of marine fishes: contemporary issues and emerging concepts. Ecol Lett 14:1288–1299

Largier JL (2004) The importance of retention zones in the dispersal of larvae. Am Fish Soc Symp 42:105–122

Largier JL, Lawrence CA, Roughan M, Kaplan DM and others (2006) WEST: A northern California study of the role of wind-driven transport in the productivity of coastal plankton communities. Deep-Sea Res II 53: 2833–2849

Lindley ST, Grimes CB, Mohr MS, Peterson W and others (2009). What caused the Sacramento River fall Chinook stock collapse? Report to the Pacific Fishery Management Council, NOAA, Portland, OR

Link J (2010) Ecosystem-based fisheries management: confronting tradeoffs. Cambridge University Press, New York, NY

Marinovic BB, Croll DA, Gong N, Benson SR, Chavez FP (2002) Effects of the 1997–1999 El Niño and La Niña events on zooplankton abundance and euphausiid community composition within the Monterey Bay coastal upwelling system. Prog Oceanogr 54:265–277

Mills KL, Laidig T, Ralston S, Sydeman WJ (2007) Diets of top predators indicate juvenile rockfish (*Sebastes* spp.) abundance in the California Current System. Fish Oceanogr 16:273–283

Moore AM, Arango HG, Broquet G, Edwards C and others (2011) The Regional Ocean Modeling System (ROMS) 4-dimensional variational data assimilation systems: Part III — Observation impact and observation sensitivity in the California Current System. Prog Oceanogr 91:74–94

Myers N, Mittermeier RA, Mittermeier CG, da Fonseca GAB, Kent J (2000) Biodiversity hotspots for conservation priorities. Nature 403:853–858

Nur N, Jahncke J, Herzog MP, Howard J and others (2011) Where the wild things are: predicting hotspots of seabird aggregations in the California Current System. Ecol Appl 21:2241–2257

Ohman MD (1984) Omnivory by *Euphausia pacifica*: the role of copepod prey. Mar Ecol Prog Ser 19:125–131

Papastephanou KM, Bollens SM, Slaughter AM (2006) Cross-shelf distribution of copepods and the role of event-scale winds in a northern California upwelling zone. Deep-Sea Res II 53:3078–3098

Polovina J, Uchida I, Balazs G, Howell EA, Parker D, Dutton P (2006) The Kuroshio Extension Bifurcation Region: a pelagic hotspot for juvenile loggerhead sea turtles. Deep-Sea Res II 53:326–339

Powell TM, Lewis CVW, Curchitser EN, Haidvogel DB, Hermann AJ, Dobbins EL (2006) Results from a three-dimensional, nested biological-physical model of the California Current System and comparisons with statistics from satellite imagery. J Geophys Res 111:C07018, doi:10.1029/2004JC002506

R Development Core Team (2013) R: a language and environment for statistical computing. R Foundation for Statistical Computing, Vienna. www.r-project.org

Reilly CA, Echeverria TW, Ralston S (1992) Interannual variation and overlap in the diets of pelagic juvenile rockfish (genus: *Sebastes*) off Central California. Fish Bull 90: 505–515

Sakuma KM, Ralston S, Wespestad VG (2006) Interannual and spatial variation in the distribution of young-of-the-year rockfish (*Sebastes* spp.): expanding and coordinating a survey sampling frame. Calif Coop Ocean Fish Invest Rep 47:127–139

Santora JA, Reiss CS, Loeb VJ, Veit RR (2010) Spatial association between hotspots of baleen whales and demographic patterns of Antarctic krill *Euphausia superba* suggests size-dependent predation. Mar Ecol Prog Ser 405:255–269

Santora JA, Sydeman WJ, Schroeder ID, Wells BK, Field JC (2011a) Mesoscale structure and oceanographic determinants of krill hotspots in the California Current: Implications for trophic transfer and conservation. Prog Oceanogr 91:397–409

Santora JA, Ralston S, Sydeman WJ (2011b) Spatial organization of krill and seabirds in the central California Current. ICES J Mar Sci 68:1391–1402

Santora JA, Sydeman WJ, Schroeder ID, Reiss CS and others (2012) Krill space: a comparative assessment of mesoscale structuring in polar and temperate marine ecosystems. ICES J Mar Sci 69:1317–1327

Santora JA, Sydeman WJ, Messié M, Chai F and others (2013) Triple check: observations verify structural realism of an ocean ecosystem model. Geophys Res Lett 40: 1367–1372

Simmonds E, MacLennan D (2005) Observation and measurement of fish. In: Pitcher TJ (ed) Fisheries acoustics: theory and practice. Blackwell Science, Oxford, p 163–215

Smith ADM, Brown CJ, Bulman CM, Fulton EA and others (2011) Impacts of fishing low-trophic level species on marine ecosystems. Science 333:1147–1150

Southwest Fisheries Science Center (2008) Management of krill as an essential component of the California Current ecosystem. Amendment 12 to the Coastal Pelagic Species Fishery Management Plan, NOAA, Portland, OR

Strub PT, Kosro PM, Huyer A (1991) The nature of cold filaments in the California Current System. J Geophys Res C 96:14743–14768

Suryan RM, Santora JA, Sydeman WJ (2012) New approach for using remotely sensed chlorophyll *a* to identify seabird hotspots. Mar Ecol Prog Ser 451:213–225

Sydeman WJ, Brodeur RD, Grimes CB, Bychkov AS, McKinnell S (2006) Marine habitat 'hotspots' and their use by migratory species and top predators in the North Pacific Ocean: introduction. Deep-Sea Res II 53:247–249

Tanasichuk RW (1999) Interannual variation in the availability and utilization of euphausiids as prey for Pacific hake (*Merluccius productus*) along the south-west coast of Vancouver Island. Fish Oceanogr 8:150–156

Torres JJ, Childress JJ (1983) Relationship of oxygen-consumption to swimming speed in *Euphausia pacifica*.1. Effects of temperature and pressure. Mar Biol 74:79–86

Vander Woude AJ, Largier JL, Kudela RM (2006) Nearshore retention of upwelled waters north and south of Point Reyes (northern California)—Patterns of surface temperature and chlorophyll observed in CoOP WEST. Deep-Sea Res II 53:2985–2998

Visser AW (1997) Using random walk models to simulate the vertical distribution of particles in a turbulent water column. Mar Ecol Prog Ser 158:275–281

Watkins J, Brierley A (2002) Verification of the acoustic techniques used to identify Antarctic krill. ICES J Mar Sci 59: 1326–1336

Wing SR, Botsford LW, Ralston SV, Largier JL (1998) Meroplanktonic distribution and circulation in a coastal retention zone of the northern California upwelling system. Limnol Oceanogr 43:1710–1721

Wingfield DK, Peckham SH, Foley DG, Palacios DM and others (2011) The making of a productivity hotspot in the coastal ocean. PLoS ONE 6:e27874

Wood S (2006) On confidence intervals for generalized additive models based on penalized regression splines. Aust NZ J Stat 48:445–464

Yen PPW, Sydeman WJ, Hyrenbach KD (2004) Marine bird and cetacean associations with bathymetric habitats and shallow-water topographies: implications for trophic transfer and conservation. J Mar Syst 50:79–99

Yen PPW, Sydeman WJ, Bograd SJ, Hyrenbach KD (2006) Spring-time distributions of migratory marine birds in the southern California Current: Oceanic eddy associations and coastal habitat hotspots over 17 years. Deep-Sea Res II 53:399–418

Editorial responsibility: Alejandro Gallego, Aberdeen, UK

Submitted: August 14, 2014; Accepted: February 24, 2015
Proofs received from author(s): May 8, 2015